



Micro-supercapacitor characteristics using a micro-ring space-time control circuit

A. E. Arumona^{1,2,3} · A. Garhwal⁴ · S. Punthawanunt⁵ · P. Youplao⁶ · K. Ray⁷ · P. Yupapin^{1,2}

Received: 2 June 2020 / Accepted: 27 November 2020

© The Author(s), under exclusive licence to Springer Science+Business Media, LLC part of Springer Nature 2021

Abstract

A micro-ring space-time control circuit is proposed for micro-supercapacitor application. The center micro-ring circuit consists of sandwiched titanium dioxide (TiO₂) thin film. The input light fed into the circuit via the input port is of 1.55 μm wavelength. The input space source is multiplexed with time at the add port to form the space-time function. A whispering-gallery mode is formed using suitable parameters, which results from the nonlinearity effect induced by the small rings at the sides of the center micro-ring. The light that excites the gold metal surface leads to electron cloud oscillations that form the electron density, which can be transported via wireless connection by employing the whispering-gallery mode or via cable connection. Areal specific capacitance of 0.4 F cm⁻² and areal power density of 0.31 MW cm⁻² are obtained. In application, the micro-ring circuit can be employed in microsystems that require high specific capacitance and high power for their operations.

Keywords Micro-supercapacitor · Specific capacitance · Micro-ring circuit · Space-time control

1 Introduction

A supercapacitor is an electric storage device with high specific capacitance and low voltage. It is a type of capacitor and is usually known as an ultracapacitor. It can charge/discharge rapidly. Supercapacitors have three general forms [1]. The first

form is the double-layer capacitor, where charges are stored electrostatically. The second form is the pseudocapacitor, where charges are stored electrochemically, while the third form is the hybrid capacitor, where charges are stored both electrostatically and chemically. The supercapacitor comes in different physical sizes and scales including micro and nano sizes. The specific capacitance of a supercapacitor can be mass specific capacitance, areal specific capacitance, or volumetric specific capacitance [2], depending on the size. Yun et al. [3] fabricated a micro-supercapacitor based on carbon material and reduced graphene oxide film. A one-step laser curving technique was employed for the fabrication. A frequency range of 0.01 Hz to 100 kHz was employed for the study, and a time range of 0–150 s was observed. Areal specific capacitance of 37.95 mF cm⁻² was obtained. Yu et al. [4] developed a flexible micro-supercapacitor based on graphene material. A laser preparation technique was employed for the fabrication, with a frequency range of 0.01 Hz to 10 kHz and a time range of 0–22,500 s. Areal specific capacitance of 2412.2 mF cm⁻² was obtained. Bencheikh et al. [5] developed a nanowire/nanoparticle micro-supercapacitor using silicon and ruthenium for the nanowire and nanoparticle material, respectively. Electroless and vapor–liquid–solid techniques were used. A frequency range of 0.03 Hz to 1 MHz was employed, and a time range of 0.1800 s was observed. An areal specific capacitance of

✉ P. Yupapin
preecha.yupapin@tdtu.edu.vn

¹ Computational Optics Research Group, Advanced Institute of Materials Science, Ton Duc Thang University, District 7, Ho Chi Minh City, Vietnam

² Faculty of Applied Sciences, Ton Duc Thang University, District 7, Ho Chi Minh City, Vietnam

³ Division of Computational Physics, Institute for Computational Science, Ton Duc Thang University, Ho Chi Minh City, Vietnam

⁴ Amity School of Engineering and Technology, Amity University Rajasthan, Jaipur, India

⁵ Faculty of Science and Technology, Kasem Bundit University, Bangkok 10250, Thailand

⁶ Rajamangla University of Technology, Isan Sakon Nakhon Campus, Sakon Nakhon 47160, Thailand

⁷ Amity School of Applied Sciences, Amity University Rajasthan, Jaipur, India

36.25 mF cm⁻² was obtained. Zhang et al. [6] developed a micro-supercapacitor based on titanium carbide material, using vacuum filtration and laser cutting techniques. A frequency range of 0.1 Hz to 100 kHz was employed, while the time range was 0–400 s. An areal specific capacitance of –19 mF cm⁻² was obtained. Feng et al. [7] developed a micro-supercapacitor based on a graphene network. Mask-free pattern and chemical vapor deposition techniques were used, with a frequency range of 0.01 Hz to 100 kHz and a time range of 0–100 s. An areal specific capacitance of 0.75 mF cm⁻² was obtained. Yang et al. [8] fabricated a micro-supercapacitor based on carbon material. A facile approach was employed for the fabrication of the micro-supercapacitor, using a frequency range of 0.01 Hz to 500 kHz and a time range of 0–320 s. An areal specific capacitance of 13.7 mF cm⁻² was obtained. In this work, a space-time control circuit is employed for micro-supercapacitor applications. The space-time control consists of a center micro-ring with a sandwiched thin film that is based on titanium dioxide (TiO₂). Compared with other works mentioned above, a frequency range of 200–600 THz is employed for this study and a time range of 0–5.10 fs is observed. The space-time function control [9, 10] is employed for the operation of the circuit for the micro-supercapacitor application. The OptiFDTD program is employed as a first step in simulating the micro-ring circuit and the whispering-gallery mode (WGM) [11, 12] from where parameters will be extracted. The Matlab program employs the extracted parameters from the OptiFDTD program and simulates the micro-ring circuit using the space-time control for supercapacitor characteristics.

2 Theoretical background

The micro-ring space-time circuit is shown in Fig. 1. The input space source is given in Eq. (1) as [13]:

$$E_{in} = E_o \cdot \exp(-ik_z z) \quad (1)$$

where $k_z = \frac{2\pi}{\lambda}$ is the wave number and λ is the input wavelength. The amplitude is given as E_o and the propagation distance as z . The space-time function is given as:

$$E_{add} = S \cdot e^{\pm i\omega t} \quad (2)$$

where $e^{\pm i\omega t}$ is the control time, and \pm indicates both sides of time. The Drude model [14] describes the behavior of the electrons in the gold metal, as given in Eqs. (3) and (4) as:

$$\epsilon(\omega) = 1 - \frac{ne^2}{\epsilon_o m \omega^2} \quad (3)$$

where ϵ_o , n , m , e and ω are relative permittivity, electron density, electron mass, electron charge, and angular frequency. At resonance, angular frequency becomes plasma frequency:

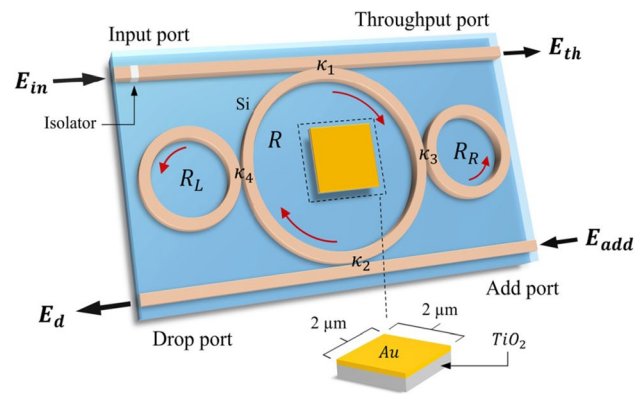


Fig. 1 The space-time control circuit. At the center is sandwiched TiO₂ thin film, where the top layer is gold metal and the bottom is silicon substrate. E_{in} is the input port, E_d is the drop port, E_{th} is the throughput port, and E_{add} is the add port. R indicates the center ring, R_R is the right small ring, and R_L is the left small ring. K_1 – K_4 are the coupling coefficients. An isolator is applied to protect the feedback

$$\omega_p = \left[\frac{ne^2}{\epsilon_o m} \right]^{\frac{1}{2}} \quad (4)$$

where Eq. (4) gives the relation of electron density $n = \frac{\omega_p^2}{e^2} \epsilon_o m$. The Kerr effect which is the nonlinear effect, where $n = n_o + n_2 I = n_o + n_2 P / A_{eff}$ is the variably the refractive equation, where n_o is the linear refractive index and n_2 is the nonlinear refractive index. I and P are the optical intensity and power, respectively. A_{eff} is the effective core area. The normalized intensities are written as:

$$\frac{I_{th}}{I_{in}} = \left[\frac{E_{th}}{E_{in}} \right]^2 \quad (5)$$

$$\frac{I_{drop}}{I_n} = \left[\frac{E_{drop}}{E_{in}} \right]^2 \quad (6)$$

The output fields of the micro-ring circuit are described as [15]:

$$E_{th} = m_2 E_{in} + m_3 E_{ad} \quad (7)$$

$$E_{dr} = m_5 E_{ad} + m_6 E_{in} \quad (8)$$

where the terms in (7) and (8) are defined in the given reference. Equation (9) gives the capacitance of the micro-supercapacitor circuit, which is inversely proportional to the frequency. The motivation for using this equation is based on the input space source (given in Eq. 1) which has an input wavelength of 1.55 μ m and travels with the speed of light.

$$C = \frac{I}{V_f} \tag{9}$$

where I is the current, V is the voltage, f is the frequency, and $f = \frac{c}{\lambda}$, c is the speed of light. Equation (10) gives the areal specific capacitance of the micro-supercapacitor circuit, which is inversely proportional to the area of the metal contact. The motivation for using this equation is based on the materials employed for the micro-supercapacitor, which in this case are the gold metal and TiO_2 thin film, where only the area is considered. The areal specific capacitance is given as [3]:

$$SC_{\text{areal}} = \frac{I\Delta t}{A\Delta V} \tag{10}$$

where I is the discharge current, Δt is the discharge time, A is the area of the metal contact, and ΔV is the voltage window. Equation (11) gives the areal energy density, where the voltage window is the difference between the final voltage discharge and initial voltage discharge. Equation (12) gives the areal power density, which is directly proportional to the areal energy density, where the discharge time is also the time constant of the micro-supercapacitor. The areal energy density and areal power density [3] are given as:

$$E_a = \frac{SC_{\text{areal}}\Delta V^2}{7200} \tag{11}$$

$$P_a = \frac{E_a(3600)}{\Delta t} \tag{12}$$

3 Results and discussion

The micro-supercapacitor system consisting of gold metal at the top, TiO_2 thin film in the middle, and silicon at the bottom, as shown in Fig. 1, is designed and simulated by the OptiFDTD version 12 program [16] in the first step. The grid size is implemented automatically for the simulation program. The micro-supercapacitor system is fed with input light of $1.55 \mu\text{m}$ wavelength via the input port. The small rings at the sides of the center micro-ring act as phase modulators and induce the nonlinearity effect in the micro-ring circuit. The nonlinearity effect of two side rings results in a small increase in terms of the optical path length of the light pulses (trapped electrons) in the center micro-ring, where the WGM is formed as shown in Fig. 2a, and the generation of plasmons in the WGM formed with electrons at the gold surface propagating with the intense electric field as shown in Fig. 2b. The suitable parameters are given in Table 1. The number of time steps is 20,000 for resonant results to

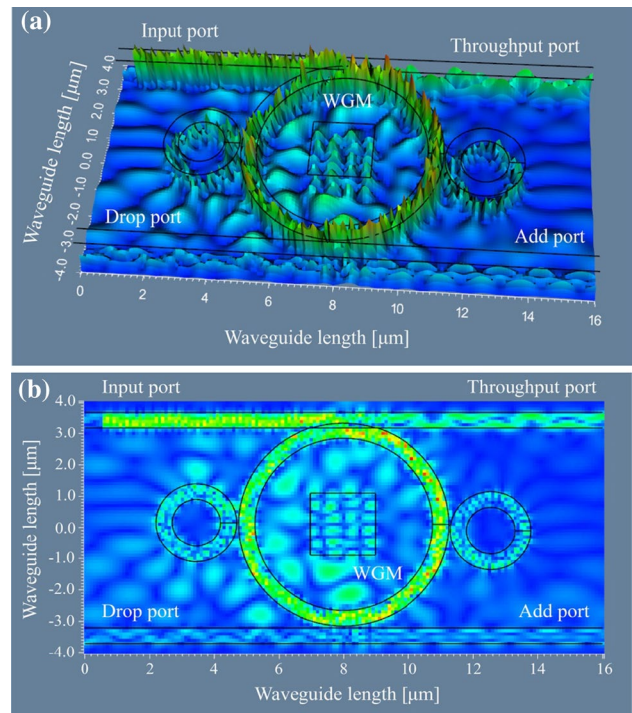


Fig. 2 Plot of the OptiFDTD results: **a** the whispering-gallery mode formed by using suitable parameters as given in Table 1; **b** the plasmons propagating in the circuit

be achieved in the simulation. The Matlab program employs the extracted parameters from the simulation results of the OptiFDTD program to simulate the micro-supercapacitor circuit characteristics. The micro-supercapacitor system is described by Eqs. (7) and (8), where the operation of the circuit is based on the space-time function. The space-time function resulting from the input space source (as given in Eq. (1)) via the input port is multiplexed with the time at the add port as given in Eq. (2), and at the output ports, the normalized electron density (as given in Eqs. (5) and (6)) is obtained. Figure 3 shows the plot of the output of the system in the wavelength and frequency domains.

The spin-up and spin-down of electrons result from the trapped electron density $[n = \frac{\omega^2}{e^2} \epsilon_0 m]$ within the micro-supercapacitor, which is formed when the WGM of light illuminates the gold metal, leading to the trapped electron cloud transport in the circuit. From Table 1, the conductivity of Mott's type is applied, which is well explained in [14]. The resistivity obtained from the relation is $\rho = 1/\sigma$. The resistance, voltage, and current are obtained from the relations $R = \frac{\rho d}{A}$, $P = V^2/R$, $P = I^2 R$, where input power (P) of 500 mW is used, and the thickness (d) of the TiO_2 thin film employed is 230 nm, which is used for the Mott conductivity of the TiO_2 thin film. Figure 4a, b is the plot of the areal specific capacitance in the wavelength and frequency domains, respectively. The areal specific capacitance is given in

Table 1 The selected simulation parameters

Parameters	Symbols	Values	Units
Input power	P	500	mW
Silicon linear waveguide length	L	16.0	μm
Silicon center ring radius	R	3.0	μm
Left nano-ring radius	R_L	1.0	μm
Right nano-ring radius	R_R	1.0	μm
Gold metal area	A	4.0×10^{-8}	cm^2
TiO ₂ thickness [17]	d	230	nm
TiO ₂ conductivity [17]	σ	4.79×10^9	$(\Omega \text{ cm})^{-1}$
TiO ₂ resistivity	ρ	2.09×10^{-10}	$\Omega \text{ cm}$
TiO ₂ refractive index [18]	n	2.11	
Coupling coefficient	κ	0.06–0.7	
Insertion loss	γ	0.50	dB mm ⁻¹
Au refractive index [19]	n	1.80	
Si refractive index [20]	n_{Si}	3.42	
Si nonlinear refractive index [20]	n_2	1.3×10^{-13}	m ² W ⁻¹
Input light wavelength	λ	1.55	μm
Plasma frequency	ω_p	1.299×10^{16}	rad s ⁻¹
Core effective area [20]	A_{eff}	0.30	μm^2
Free space permittivity	ϵ_o	8.85×10^{-12}	Fm ⁻¹
Electron mass	m	9.11×10^{-31}	kg
Electron charge	e	1.60×10^{-19}	Coulomb
Waveguide loss	α	0.50	dB (mm) ⁻¹

Eq. (10), where the capacitance is obtained from Eq. (9). The areal specific capacitance increases as the wavelength increases, and it decreases as the frequency increases. Optimum areal specific capacitance of 0.4 F cm^{-2} is obtained. Employing Eqs. (11) and (12) Fig. 5a shows the plot of areal energy density and areal power density, where the optimum areal energy density obtained is 25 pWh cm^{-2} , while the optimum areal power density obtained is 0.31 MW cm^{-2} . The areal energy density increases as the areal power density increases. The areal energy density is directly proportional to the areal power density. Figure 5b shows the plot of the relationship between the current and voltage. The relationship is linear. The optimum current obtained is 2.5 kA, while the optimum voltage obtained is 0.25 mV. Figure 6 is the plot of the areal specific capacitance in the time domain. The time taken to reach the optimum areal specific capacitance of 0.4 F cm^{-2} is 5.10 fs.

4 Conclusion

A micro-ring circuit is proposed and manipulated for a micro-supercapacitor application. The working principle of the circuit is based on space-time control. The input space source fed into the system via the input port is

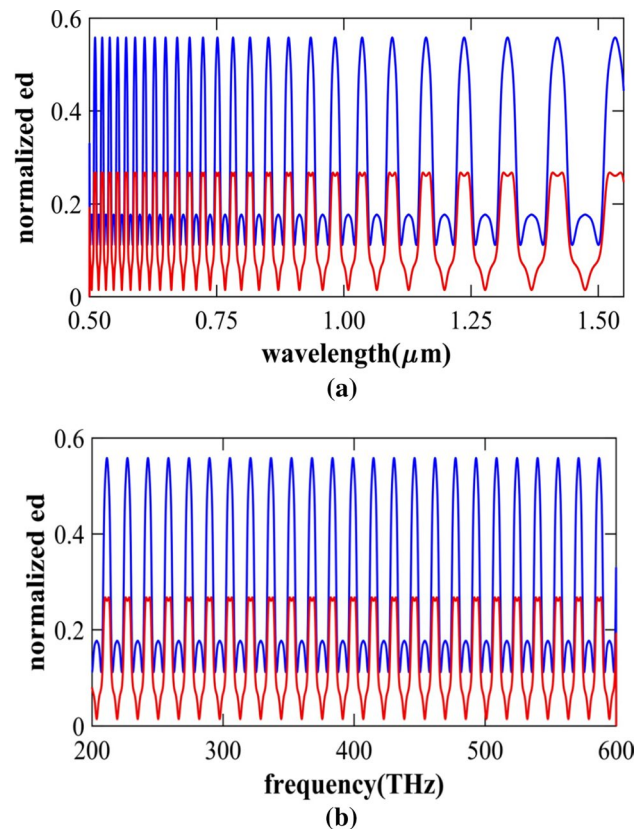


Fig. 3 Plot of the output of the circuit: **a** wavelength domain and **b** frequency domain. The vertical axis is the normalized electron density (unitless)

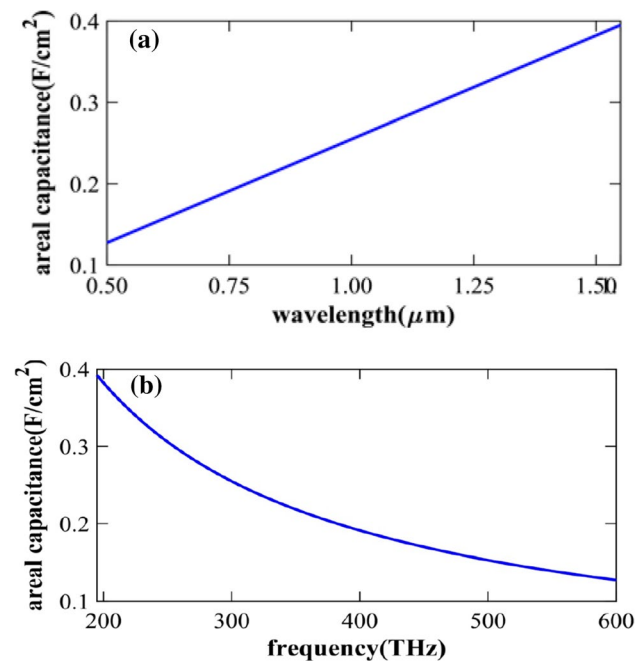


Fig. 4 Plot of the areal specific capacitance: **a** wavelength domain, **b** frequency domain. The optimum areal specific capacitance of 0.4 F cm^{-2} is obtained

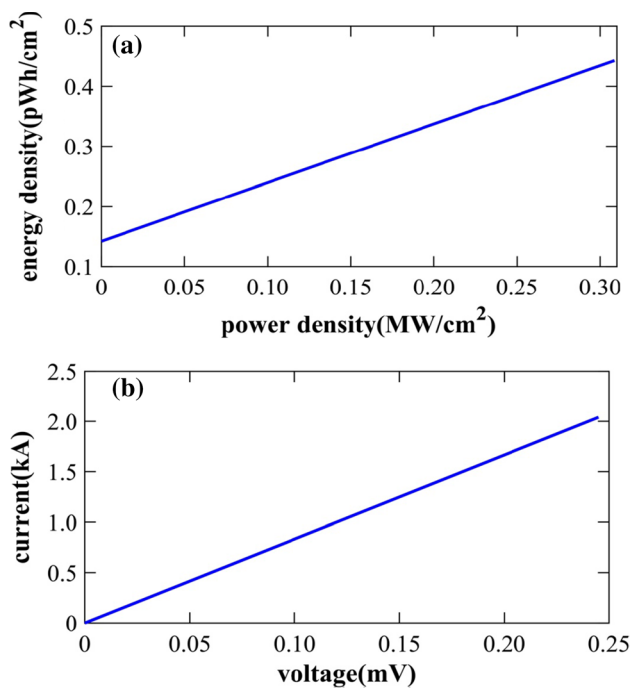


Fig. 5 Plot of **a** areal energy density and areal power density; the optimum areal energy density obtained is 25 pWh cm^{-2} , while the optimum areal power density obtained is 0.31 MW cm^{-2} . **b** Current and voltage. The optimum current obtained is 2.5 kA , while the optimum voltage obtained is 0.25 mV

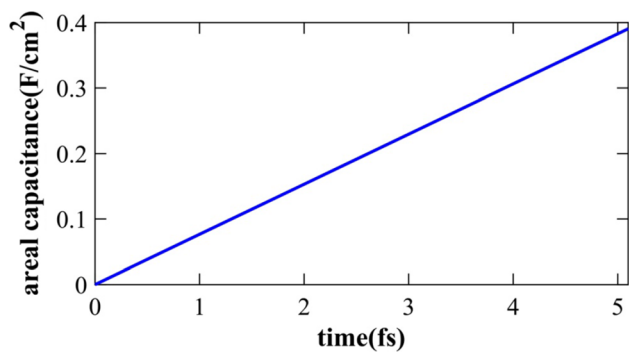


Fig. 6 Plot of the areal specific capacitance and time. The time taken to reach the maximum areal specific capacitance is 5.10 fs

multiplexed with time at the add port. When light illuminates the metal surface, the electron densities formed can be transported via wireless connection by employing the whispering-gallery mode or by cable connection. Areal specific capacitance of 0.4 F cm^{-2} , areal energy density of 25 pWh cm^{-2} , and areal power density of 0.31 MW cm^{-2} are obtained. The micro-ring circuit can be applied in microsystems that require high specific capacitance and high power for their operation.

Acknowledgements The authors would like to acknowledge the research facilities from Ton Duc Thang University, Vietnam.

Authors' contributions A.E. Arumona: Matlab results improvement, review and editing, and discussion, A. Garhwal: Graphic improvement and discussion, S. Punthawanunt: Discussion and English polishing, P. Youplao: Validation, comparing OptiFDTD and Matlab results, visualization, and discussion, K. Ray: Modeling, analysis, discussion, and final editing, P. Yupapin: Conceptualization, supervision, review, editing and submission. All authors have read through the manuscript.

Funding This research is funded by the Foundation of Science and Technology Development of Ton Duc Thang University (FOSTECT), website: <http://fostect.tdtu.edu.vn>, under the research grant number FOSTECT.2017.BR.07.

Availability of data and materials Not applicable.

Compliance with ethical standards

Conflict of interest The authors have declared no conflict of interest.

Ethical approval Not applicable.

Consent to participate All authors are pleased to participate in this article.

Consent to Publish All authors give consent to publish this article.

References

- Davis, A.K., Gunasekaran, M.K.: Microprocessor-conducted noise reduction with switched supercapacitors. *Electron. Lett.* **51**(1), 92–94 (2015)
- Freeborn, T.J.: Estimating supercapacitor performance for embedded applications using fractional order models. *Electron. Lett.* **52**(17), 1478–1480 (2016)
- Yun, X., Xiong, Z., Tu, L., Bai, L., Wang, X.: Hierarchical porous graphene film: an ideal material for laser-carving fabrication of flexible micro-supercapacitor with high specific capacitance. *Carbon* **125**, 308–317 (2017)
- Yu, X., et al.: Ultra-thick 3D graphene frameworks with hierarchical pores for high performance flexible micro-supercapacitors. *J. Power Sources* **478**, 229075 (2020)
- Bencheikh, Y., et al.: High performance silicon nanowires/ruthenium nanoparticles micro-supercapacitors. *Electrochim. Acta* **311**, 150–159 (2019)
- Zhang, L., et al.: Mxene coupled with molybdenum dioxide nanoparticles as 2D-0D pseudocapacitive electrode for high performance flexible asymmetric micro-supercapacitors. *J. Materiomics* **6**(1), 138–144 (2020)
- Feng, X., et al.: All-solid state planner micro-supercapacitor based on graphene/NiOOH/Ni(OH)₂ via mask-free patterning strategy. *J. Power Sources* **418**, 130–137 (2019)
- Yang, W., et al.: Carbon-MEMS based alternating stacked MoS₂@rGOCNT micro-supercapacitor with high capacitance and energy density. *Small* **13**(26), 1700639 (2017)
- Bunruangses, M., Arumona, A.E., Youplao, P., Pornsuwancharoen, N., Ray, K., Yupapin, P.: Modelling of a superconducting sensor with microring-embedded gold-island space-time control. *J. Comput. Electron.* **19**, 1678–1684 (2020)

10. Bunruangses, M., et al.: Microring distributed sensors using space-time function control. *IEEE Sens. J.* **20**(2), 799–805 (2020)
11. Punthawanunt, S., Aziz, M.S., Phatharacorn, P., et al.: LiFi cross-connection node model using whispering gallery mode of light in a microring resonator. *Microsyst. Technol.* **24**, 4833–4838 (2018)
12. Trong, H.B.N., Chang, Y.C.: Whispering gallery modes in hybrid AU-ZnO microsphere resonators: experimental and theoretical investigations. *Opt. Mater. Express* **7**(8), 2962–2967 (2017)
13. Arumona, A.E., Amiri, I.S., Yupapin, P.: Plasmonic micro-antenna characteristics using gold grating embedded panda-ring circuit. *Plasmonics* **15**, 279–285 (2020)
14. Tunsiri, S., Thammawongsa, N., Threepak, T., Mitatha, S., Yupapin, P.: Microring switching control using plasmonic ring resonator circuits for super-channel use. *Plasmonics* **14**, 1669–1677 (2019)
15. Prateep, P., Surasak, C., Yupapin, P.: Analytical and simulation of a triple micro whispering gallery mode probe system for a 3D blood flow rate sensor. *Appl. Opt.* **55**, 9504–9513 (2016)
16. OptiFDTD Technical Background and Tutorials (Finite Difference Time Domain) Photonics Simulation Software, Version 12.0. <http://www.optiwave.com>, Searched on 20th Sept, 2019
17. Yildiz, A., Lisesivdin, S.B., Kasap, M., Mardare, D.: Electrical properties of TiO₂ thin films. *J. Non-Cryst. Solids* **354**, 4494–4497 (2008)
18. Yu, M.E., Romashkin, S.V., Tromifov, N.S., Chekhlova, T.K.: Optical properties of TiO₂ thin film. *Phys. Procedia* **73**, 100–107 (2015)
19. Pornsuwancharoen, N., Amiri, I.S., Suhailin, F.H., Aziz, M.S., Ali, J., Singh, G., Yupapin, P.: Micro-current source generated by a WGM of light within a stacked silicon-graphene-Au waveguide. *IEEE Photon. Technol. Lett.* **29**, 1768–1771 (2017)
20. Prabhu, A.M., Tsay, A., Han, Z., Van, V.: Extreme miniaturization of silicon add-drop microring filters for VLSI photonics applications. *IEEE Photon. J.* **2**, 436–444 (2010)

Publisher's Note Springer Nature remains neutral with regard to jurisdictional claims in published maps and institutional affiliations.